

# Radiolabeling of Avidin with Very High Specific Activity for Internal Radiation Therapy of Intraperitoneally Disseminated Tumors<sup>1</sup>

Marcelo Mamede, Tsuneo Saga,<sup>2</sup>  
Hisataka Kobayashi, Takayoshi Ishimori,  
Tatsuya Higashi, Noriko Sato,  
Martin W. Brechbiel, and Junji Konishi

Department of Nuclear Medicine and Diagnostic Imaging, Graduate School of Medicine, Kyoto University, Kyoto 606-8507, Japan [M. M., T. S., H. K., T. I., T. H., N. S., J. K.], and National Cancer Institute, NIH, Bethesda, Maryland 20892 [M. W. B.]

## ABSTRACT

**Purpose:** For the effective internal radiation therapy of i.p. disseminated tumors, we developed avidin (Av)-dendrimer-chelate complex, which can be labeled with indium-111, emitting Auger and conversion electrons, with very high specific activity, and we studied its internalization, biodistribution, and therapeutic effect in nude mice with i.p. tumors.

**Experimental Design:** Generation 4 dendrimer (G4) was biotinylated and conjugated with 52 1B4M chelates. <sup>111</sup>In-G4-bt was mixed with Av to form <sup>111</sup>In-G4-Av complex. <sup>111</sup>In-G4-Av was incubated with ovarian cancer cells (SHIN-3), and the rate of internalization of the radiolabel into SHIN-3 cells was followed. <sup>111</sup>In-G4-Av was i.p. injected into nude mice that had i.p. disseminated SHIN-3 tumors, and the biodistribution was determined. Nude mice bearing i.p. disseminated tumors received i.p. injection of <sup>111</sup>In-G4-Av (9.25 or 18.5 MBq × 2, with a 1-week interval) and were followed for the formation of malignant ascites.

**Results:** Av could be labeled with <sup>111</sup>In with specific activity as high as 37 GBq/mg. More than 75% of the radioactivity was internalized 24 h after binding to cancer cells. <sup>111</sup>In-G4-Av accumulated rapidly and highly in the i.p. tumors (128.20% injected dose/gram of tissue at 2 h, 114.91% injected dose/gram of tissue at 24 h for unsaturated compound) with high tumor:background ratios. Treatment

with a high dose of <sup>111</sup>In-G4-bt-Av was tolerable and showed dose-dependent therapeutic effect.

**Conclusions:** G4-Av complex, which could be labeled with <sup>111</sup>In with very high specific activity and showed efficient internalization into cancer cells and high accumulation to i.p. tumors, appears to be suitable for the internal radiation therapy of i.p. disseminated tumors using metallic radionuclides emitting Auger and conversion electrons.

## INTRODUCTION

Peritoneal carcinomatosis is characterized as the spread and implantation of cancer cells throughout the peritoneal cavity, which arises from malignancies that originate primarily in the peritoneum (1, 2), as well as from gastrointestinal and gynecological tumors (3) and others. This is an advanced stage in cancer progression, and it can hardly be controlled by a single treatment strategy or a combination of traditional treatment strategies. Selective targeting of therapeutic agents appears to be a promising therapeutic modality for these disseminated lesions (4–6). Development of an ideal vehicle to carry therapeutic agents selectively to the target has long been awaited.

Starburst PAMAM<sup>3</sup> dendrimers are a new class of highly branched spherical polymers that are highly soluble in aqueous solution and have a unique surface of primary amino groups (7, 8). Compared with many other types of already synthesized dendritic macromolecules, PAMAM dendrimers are undispersed and show high charge densities restricted to the surface of the molecule (9). The defined structure and large number of surface amine groups have led PAMAM dendrimers to be used as a substrate for the attachment of multiple chelating agents to antibodies, contrast agent, and radiopharmaceuticals (10–14). Due to the polycationic surface of the dendrimers, the electrostatic interaction with negatively charged residues on the cell surface is believed to trigger the endocytosis process.

Av is a  $M_r$  67,000 natural, highly glycosylated (terminal *N*-acetylglucosamine and mannose residues) polycationic protein of egg white (15). This protein shows extremely high binding affinity with biotin (16). Av, when injected i.v., makes complexes with biotinylated antibody in the circulation and has been used to remove nonbound biotinylated antibodies from the circulation in tumor imaging studies (17–19). On the other hand, when injected i.p., radiolabeled Av is localized and internalized highly and rapidly in i.p. tumors and is associated with rapid blood clearance (20, 21). It has been reported that the carbohy-

Received 12/27/02; revised 3/28/03; accepted 4/1/03.

The costs of publication of this article were defrayed in part by the payment of page charges. This article must therefore be hereby marked *advertisement* in accordance with 18 U.S.C. Section 1734 solely to indicate this fact.

<sup>1</sup>Supported by Grants-in-Aid for Scientific Research 12470188 from the Ministry of Education, Culture, Sports, Science and Technology of Japan.

<sup>2</sup>To whom requests for reprints should be addressed, at Department of Nuclear Medicine and Diagnostic Imaging, Graduate School of Medicine, Kyoto University, 54 Kawahara-cho, Shogoin, Sakyo-ku, Kyoto 606-8507, Japan. Phone: 81-75-751-3419; Fax: 81-75-771-9709; E-mail: saga@kuhp.kyoto-u.ac.jp.

<sup>3</sup>The abbreviations used are: PAMAM, polyamidoamine; Av, avidin; ID/g, injected dose per gram of tissue; CE, conversion electron; LET, linear energy transfer; HABA, 2-(4'-hydroxyazobenzene) benzoic acid; Bt, biotin.

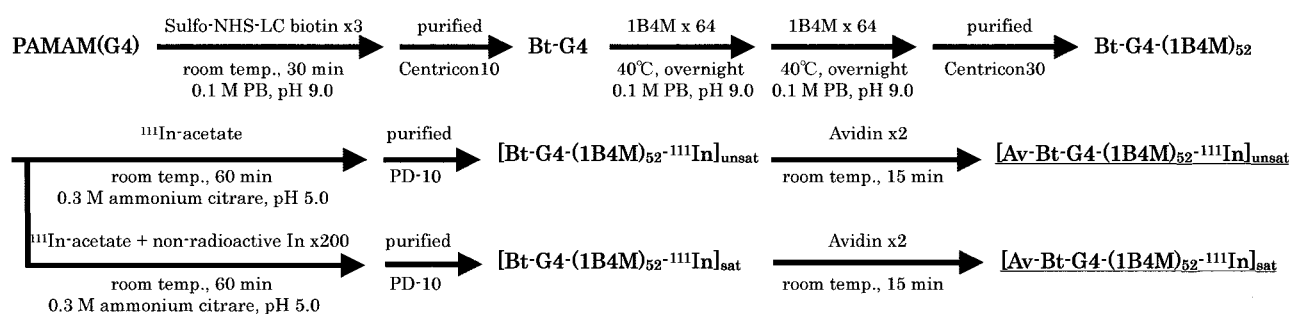


Fig. 1 Flow chart of the protocol for preparing Av-Bt-G4-(1B4M)<sub>52</sub>-<sup>111</sup>In.

drate moiety of Av contributes to tumor and liver accumulations by some specific carbohydrate binding sites (lectins) (16, 21, 22).

Internal radiation therapy using cancer-specific agents labeled with high-energy  $\beta$ -emitters can theoretically deliver a radiation dose selectively to cancer tissues. However, because of the nonspecific distribution in normal organs and the long path length of high-energy  $\beta$ -rays, there will be significant radiation exposure to normal organs, which is dose-limiting and degrades the therapeutic effect. In contrast, cancer-specific agents labeled with low-energy Auger and/or CE emitters, which bind and internalize selectively into the cancer cells, could be used as alternatives to those labeled with  $\beta$ -emitters (23–27). Auger/CE emitters have a short path length, and the ionization density within this range resembles the pattern of  $\alpha$ -particles or other high LET radiations (28). Therefore, Auger/CE emitters could be extremely effective for cancer therapy if suitable carrier agents can be made to deliver Auger/CE emitters close enough to the nucleus. In cancer-specific agents, internalization occurs only after specific binding to cancer cells, and it may not happen after nonspecific accumulation in normal organs and therefore may not cause significant damage to the normal organs. Furthermore, nonspecific radiation damage to the hematopoietic cells by circulating agents labeled with Auger/CE emitters is negligible because of the very short path length of Auger/CE electrons.

Thus, the ideal agent to treat peritoneal carcinomatosis effectively appears to be (a) an agent that can deliver a large amount of Auger/CE emitters to the disseminated tumors (*i.e.* can be labeled with Auger/CE emitters with very high specific activity), (b) an agent that internalizes after binding to cancer cells and delivers the radionuclide close to the nucleus, and (c) an agent that accumulates little in normal organs. In this study, we synthesized a compound using dendrimer and Av that was radiolabeled with a very high specific activity of Auger/CE electron emitter (<sup>111</sup>In), and we evaluated its internalization, biodistribution, and therapeutic effect in mice bearing an *i.p.* disseminated tumor. Internalization and biodistribution were studied for both saturated and unsaturated compound because the degree of occupancy of chelating sites may affect the behavior of the radiolabeled compound.

## MATERIALS AND METHODS

**PAMAM Dendrimers.** In this study, the generation 4 PAMAM dendrimer (G4) was used. G4 has an ethylenediamine

core that possesses 64 reactive amino groups on its surface and has a molecular weight of 14,215 (Sigma-Aldrich Chemical Co., Milwaukee, WI).

**Biotinylation and Conjugation of Chelates to Dendrimer.** A brief description of the method and the final complex achieved are shown in Fig. 1. At room temperature, 10 mg of G4 [0.7  $\mu$ mol in 1 ml of 0.1 M phosphate buffer (pH 9.0)] were mixed for 30 min with 2.1  $\mu$ mol of Bt (sulfo-NHS-LC-biotin;  $M_r$  556; Pierce Chemical Co., Rockford, IL) at a molar ratio of 1:3. The mixture was applied to a diafiltration membrane (Centricon 10; Amicon, Inc., Beverly, MA) to remove unbound Bt. After purification, a small aliquot of biotinylated G4 (Bt-G4) was examined with a modified HABA assay (15, 17). In brief, the HABA reagent (Pierce Chemical Co.) was prepared according to the manufacturer's instructions by adding 10 mg of Av and 600  $\mu$ l of 10 mM HABA to 19.4 ml of PBS. One hundred  $\mu$ l of diluted Bt-G4 solution were added to 900  $\mu$ l of Av-HABA solution. Then, the absorbance was measured at 500 nm. Approximately 2.5 biotin molecules were conjugated to a single G4 molecule.

Purified G4-Bt (5.95  $\mu$ g) was reacted with a 64-fold molar excess (26.78  $\mu$ mol) of 2-(*p*-isothiocyanatobenzyl)-6-methyldiethylenetriaminepentaacetic acid chelate (1B4M;  $M_r$  555; Ref. 29) at 40°C and maintained at pH 9.0 with 1 M NaOH for 24 h. An additional amount of 1B4M was added as a solid 24 h later at the same molar ratio, and the same pH was maintained for another 24 h.

The resulting compound was purified by diafiltration using Centricon 30 (Amicon Co.). Approximately 51.75 1B4M molecules were conjugated to the amine groups (80.9% of the binding sites) on the single dendrimer molecule [Bt-G4-(1B4M)<sub>52</sub>], as determined by <sup>111</sup>In labeling of the reacted sample as described previously (12). In brief,  $\sim$ 500,000 cpm ( $\sim$ 0.4 pmol) of <sup>111</sup>In-acetate was added to  $\sim$ 100  $\mu$ g/10  $\mu$ l of the conjugate samples before diafiltration and incubated in 0.1 M ammonium citrate for 60 min at room temperature. The fractions bound to the conjugates and free 1B4M were then separated using a PD-10 column (Amersham Pharmacia Biotech AB, Uppsala, Sweden) and counted. The number of 1B4M chelates bound to Bt-G4 was calculated from the count of the radioactivity in the fraction bound to the conjugates.

The binding ability of <sup>111</sup>In-labeled Bt-G4-(1B4M)<sub>52</sub> to the immobilized Av gel (Pierce Chemical Co.) was examined as described previously (17). In brief,  $\sim$ 50,000 cpm of Bt-G4-(1B4M)<sub>52</sub>-<sup>111</sup>In was incubated with 0.1 ml of immobilized Av

gel and 0.2 ml of PBS (pH 7.4) for 30 min at room temperature. Then the gel fraction was washed and separated from the supernatant. The radioactivity of both fractions was counted using a gamma counter (Aloka, Tokyo, Japan). This yielded >80.0% of the  $^{111}\text{In}$ -labeled Bt-G4-(1B4M) $_{52}$  bound to the immobilized Av gel.

**Radiolabeling of Bt-G4-(1B4M) $_{64}$  and Preparation of  $^{111}\text{In}$ -labeled Av-Bt-G4-(1B4M) $_{52}$ .** At room temperature, 20  $\mu\text{g}$  of Bt-G4-(1B4M) $_{52}$  was reacted with 7.4 MBq (200  $\mu\text{Ci}$ ) of  $^{111}\text{In}$ -acetate in 100  $\mu\text{l}$  of 0.3 M ammonium citrate at pH 5.0 for 60 min (12). To remove any nonincorporated free radiometal, 10  $\mu\text{l}$  of 0.05 M EDTA were added and purified using a PD-10 column, eluted with PBS (pH 7.4). The purified samples were mixed with a 2-fold molar excess of Av and incubated for 15 min at room temperature. The resulting purified material was referred to as "unsaturated" ( $[\text{Av-Bt-G4-(1B4M)}_{52}\text{-}^{111}\text{In}]_{\text{unsat}}$ ) because most of the chelating sites on this molecule were unoccupied under this condition.

In addition, the chelating sites on Av-Bt-G4-(1B4M) $_{52}$  were saturated with either radioactive or nonradioactive In(III). The preparation method was the same as that described above, except that a 200-fold molar excess of nonradioactive In(III) citrate (0.281  $\mu\text{mol}$ ; Nakalai Tesque, Tokyo, Japan) to conjugated 1B4M was added to the reaction mixture and incubated for 15 min before the addition of EDTA and subsequent purification. The radiolabeling yields of the  $[\text{Av-Bt-G4-(1B4M)}_{52}\text{-}^{111}\text{In}]_{\text{unsat}}$  and  $[\text{Av-Bt-G4-(1B4M)}_{52}\text{-}^{111}\text{In}]_{\text{sat}}$  compounds were >83.4% and ~47.0%, respectively. When  $^{111}\text{In}$  and Av-Bt-G4-(1B4M) $_{52}$  were mixed in various mixing ratios, the specific activities of the unsaturated compound ranged from 64.8 to 37,000 kBq/ $\mu\text{g}$ .

**Internalization Assay.** The human ovarian cancer cell line SHIN-3 was used to study an *in vitro* internalization assay and also used to generate i.p. disseminated tumors in mice for the biodistribution and therapeutic experiment. The SHIN-3 cells ( $3 \times 10^5$ ) were preseeded in 35-mm dishes and cultured overnight in RPMI 1640 (Nissui Pharmaceutical Co., Tokyo, Japan) supplemented with 10% FCS (Life Technologies, Inc., Grand Island, NY) and 0.03% L-glutamine in a 5%  $\text{CO}_2$  environment. Subconfluent cells were incubated with 425,000 cpm (0.02  $\mu\text{mol}$ ) of  $[\text{Av-Bt-G4(1B4M)}_{52}\text{-}^{111}\text{In}]_{\text{unsat}}$  or  $[\text{Av-Bt-G4(1B4M)}_{52}\text{-}^{111}\text{In}]_{\text{sat}}$  in 1 ml of RPMI 1640 with 10% FCS for 1 h at room temperature. The medium containing the tracers was then replaced by 1 ml of standard RPMI 1640. The cells were further cultured at 37°C and 4°C. At 0, 1, 3, 5, 10, and 24 h ( $n = 3$ ), the medium was removed, and the cells were washed with PBS (pH 7.6). The cells were then washed with acidic solution [0.05 M glycine-HCl/0.1 M NaCl (pH 2.8)]. The radioactivities in the acid-resistant (internalized) and acid-sensitive (membrane-bound) fractions were counted using an auto-well gamma counter. The percentages of the membrane-bound fraction and internalized fraction of the total added radioactivity were calculated. The assay at 4°C could be performed only up to 3 h because cells died and detached thereafter.

**Biodistribution Study.** The i.p. tumor xenografts were established by i.p. injection of SHIN-3 cells ( $3 \times 10^6$ ) suspended in 350  $\mu\text{l}$  of PBS into 5-week-old female BALB/c nude mice. Twenty days later, numerous small i.p. disseminated tumors had grown in the peritoneal cavity, especially at the

hilum of the spleen, the root of the mesenterium, and around the stomach. Two groups of i.p. tumor-bearing mice received an i.p. injection of 74 kBq of  $[\text{Av-Bt-G4-(1B4M)}_{52}\text{-}^{111}\text{In}]_{\text{unsat}}$  and  $[\text{Av-Bt-G4-(1B4M)}_{52}\text{-}^{111}\text{In}]_{\text{sat}}$  compounds. The mice were sacrificed 2, 10, and 24 h after i.p. injection by ether inhalation. Blood, i.p. disseminated tumors, and various organs were removed and weighed, and their radioactivities were determined by gamma counter. The percentages of ID/g normalized to a 20-g mouse were determined. The tumor:normal tissue uptake ratios of the radioactivity were also calculated.

**Internal Radiation Therapy of i.p. disseminated Micrometastases.** Five days after receiving an i.p. injection of SHIN-3 cells ( $3 \times 10^6$ ), two groups of treated mice received an i.p. injection of 9.25 MBq (group A) and 18.5 MBq (group B) of  $[\text{Av-Bt-G4-(1B4M)}_{52}\text{-}^{111}\text{In}]_{\text{unsat}}$  ( $n = 7$ ; specific activity 3.3 MBq/ $\mu\text{g}$ ). One week later, these mice received another i.p. injection of 9.25 and 18.5 MBq of the same compound, respectively. The evolution of tumor growth and hemorrhagic ascites was followed and compared with those of untreated mice ( $n = 7$ ).

All animal experiments were carried out in accordance with the regulations of the Kyoto University animal facility regarding animal care and handling.

**Statistical Analysis.** We performed statistical analyses using the *t* test for independent variables and Kaplan-Meier cumulative survival curves. Values were considered significant at  $P < 0.05$ .

## RESULTS

**Internalization Assay.** The human ovarian cancer SHIN-3 cells showed progressive internalization of the radioactivity when incubated at 37°C (Fig. 2), and 77.6% of the radioactivity of  $[\text{Av-Bt-G4(1B4M)}_{52}\text{-}^{111}\text{In}]_{\text{unsat}}$  and 86.0% of the radioactivity of  $[\text{Av-Bt-G4(1B4M)}_{52}\text{-}^{111}\text{In}]_{\text{sat}}$  were internalized after 24 h of incubation. The increases in the radioactivity during the internalization assay were significant for both compounds ( $P < 0.01$ , ANOVA). In contrast, when incubated at 4°C, SHIN-3 cells showed no significant internalization of radioactivity for both compounds (data not shown).

**Biodistribution Study.** The percentages of ID/g in i.p. tumor-bearing mice at 2, 10, and 24 h postinjection of  $[\text{Av-Bt-G4-(1B4M)}_{52}\text{-}^{111}\text{In}]_{\text{unsat}}$  and  $[\text{Av-Bt-G4-(1B4M)}_{52}\text{-}^{111}\text{In}]_{\text{sat}}$  compounds are shown in Tables 1 and 2.

When injected i.p., both radiolabeled compounds showed rapid and high accumulation in the i.p. disseminated tumors. Two h after injection, the tumor uptake of radioactivity reached 128.20% and 65.92% ID/g, respectively, and a high level of radioactivity remained until 24 h postinjection (114.91% and 49.28% ID/g, respectively).

The concentrations of both radiolabeled compounds (unsaturated and saturated) in the blood were considerably low (0.49% and 0.63% ID/g at 2 h, respectively), resulting in very high tumor:blood ratios (329.63 for unsaturated compound and 144.14 for saturated compound at 2 h).  $[\text{Av-Bt-G4-(1B4M)}_{52}\text{-}^{111}\text{In}]_{\text{unsat}}$  and  $[\text{Av-Bt-G4-(1B4M)}_{52}\text{-}^{111}\text{In}]_{\text{sat}}$  compounds also showed very low accumulation of radioactivity in the bone and muscle. Relatively high uptake of radioactivity was observed in stomach and spleen for both compounds, followed by liver,

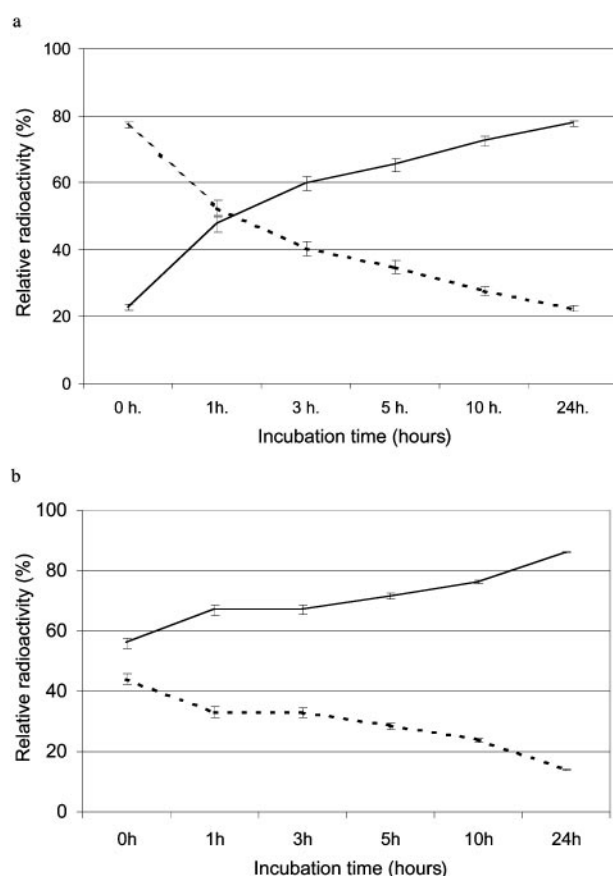


Fig. 2 Internalization assay of [Av-Bt-G4-(1B4M)<sub>52</sub>-<sup>111</sup>In]<sub>unsat</sub> (a) and [Av-Bt-G4-(1B4M)<sub>52</sub>-<sup>111</sup>In]<sub>sat</sub> (b) bound to SHIN-3 ovarian cancer cells at 37°C. Temporal changes of the percentages of the internalized (acid-resistant) radioactivity (solid line) and membrane-bound (acid-sensitive) radioactivity (dashed line) in the total bound radioactive are illustrated. Bars indicate SD of the triplicate sample.

Table 1 Biodistribution of [Av-Bt-G4(1B4M)<sub>52</sub>-<sup>111</sup>In]<sub>unsat</sub> 2, 10, and 24 h after i.p. injection in Balb/c nude mice bearing an i.p. disseminated tumor

Organs	2 h	10 h	24 h
Blood	0.49 ± 0.29 <sup>a</sup>	0.29 ± 0.24	0.40 ± 0.40
Liver	5.89 ± 1.15	5.50 ± 1.86	8.06 ± 1.05
Kidney	3.47 ± 0.38	3.59 ± 0.16	4.38 ± 1.36
Intestine	4.67 ± 1.38	3.55 ± 1.31	3.24 ± 1.64
Stomach	10.29 ± 3.08	7.67 ± 3.72	6.70 ± 3.10
Spleen	7.57 ± 2.91	6.31 ± 2.90	15.26 ± 2.54
Lung	2.11 ± 0.53	3.28 ± 4.46	11.80 ± 2.30
Muscle	1.27 ± 0.82	1.04 ± 0.79	1.48 ± 1.06
Bone	1.10 ± 0.60	1.00 ± 0.54	0.95 ± 0.15
SHIN-3	128.20 ± 17.06	116.84 ± 29.65	114.91 ± 19.59

<sup>a</sup> Values represent percentages of ID/g of tissue (mean ± SD of five mice).

lung, kidneys, and intestine. Although the radioactivities in the stomach and intestine decreased with time, uptakes in the spleen, lung, liver, and kidney showed a tendency to increase with time.

Table 2 Biodistribution of [Av-Bt-G4(1B4M)<sub>52</sub>-<sup>111</sup>In]<sub>sat</sub> 2, 10, and 24 h after i.p. injection in Balb/c nude mice bearing i.p. disseminated tumor

Organs	2 h	10 h	24 h
Blood	0.63 ± 0.45 <sup>a</sup>	0.37 ± 0.17	0.31 ± 0.07
Liver	2.47 ± 1.64	3.61 ± 0.69	5.68 ± 0.78
Kidney	2.40 ± 1.15	3.66 ± 1.07	4.35 ± 2.30
Intestine	1.42 ± 0.63	0.98 ± 0.22	1.09 ± 0.26
Stomach	3.21 ± 1.29	2.49 ± 1.02	2.27 ± 0.99
Spleen	3.00 ± 1.58	3.71 ± 0.66	8.10 ± 1.66
Lung	1.45 ± 1.03	4.73 ± 1.43	4.21 ± 1.85
Muscle	0.51 ± 0.19	0.35 ± 0.23	0.28 ± 0.04
Bone	0.62 ± 0.17	0.75 ± 0.51	0.84 ± 0.34
SHIN-3	65.92 ± 25.06	44.12 ± 11.48	49.28 ± 9.91

<sup>a</sup> Values represent percentages of ID/g of tissue (mean ± SD of five mice).

Fig. 3 compares the biodistribution of saturated and unsaturated compounds at 2 and 24 h after i.p. injection. The unsaturated compound accumulated more in disseminated tumors and in all organs, except for blood. These differences were essentially significant in most of the organs and tumors.

**Auger/CE Therapy for i.p. disseminated Micrometastases.** Body weight of the treated mice did not change after the administration of the radiolabeled compound (data not shown), and all mice could tolerate the administration of a high dose of <sup>111</sup>In-labeled compound twice, and no death related to radiotoxicity was observed. Ascites-free survival of the treated and nontreated mice was compared in Fig. 4. Without treatment, mice developed ascites about 1 month after i.p. injection of SHIN-3 cells (32.43 ± 2.99 days). In contrast, ascites-free survival was significantly longer in the treated mice (53.00 ± 3.27 days for group A and 63.14 ± 3.13 days for group B). All mice, regardless of the administered dose, appeared healthy and alert before the development of ascites.

Cumulative ascites-free survival curves for treated (groups A and B) and untreated mice are shown in Fig. 4. Compared with nontreated mice, treated mice (groups A and B) showed significantly longer ascites-free survival ( $P < 0.01$  for both). In addition, mice treated twice with 18.5 kBq (group B) survived significantly longer than those treated twice with 9.25 kBq (group A;  $P < 0.01$ ).

## DISCUSSION

Although a great number of therapeutic agents are discovered and/or created every year, their clinical applications are often limited by failure to reach the site of action. An additional problem is the toxicity of drugs toward nontarget sites. Selective drug targeting would not only reduce systemic toxicity but would also augment the efficacy of drug action by concentrating the drug in target cells or tissues.

In this study, we developed a compound that could be labeled with extremely high specific activity (theoretically, 37GBq/μg), internalized effectively into human ovarian cancer cells (86.0% and 77.6% at 24 h for saturated and unsaturated compounds, respectively), and accumulated highly and rapidly in i.p. disseminated tumor xenografted into BALB/c nude mice. When high doses of this compound were injected i.p. in these



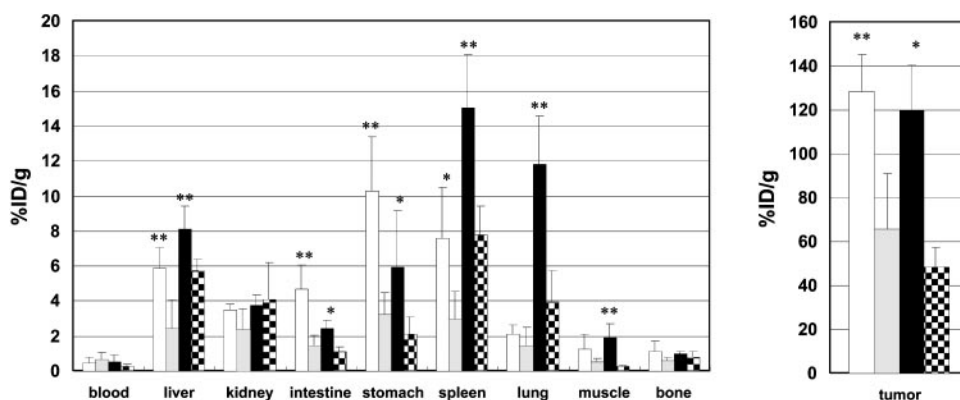


Fig. 3 Comparison of biodistribution between saturated and unsaturated compounds at 2 and 24 h after i.p. injection in BALB/c nude mice bearing an i.p. disseminated tumor. □, 2 h postinjection of the unsaturated compound; ▒, 2 h postinjection of the saturated compound; ■, 24 h postinjection of the unsaturated compound; ▣, 24 h postinjection of the saturated compound. \* represents  $P < 0.05$  between values from unsaturated and saturated compounds at 2 or 24 h postinjection; \*\* represents  $P < 0.01$  between values from unsaturated and saturated compounds at 2 or 24 h postinjection.

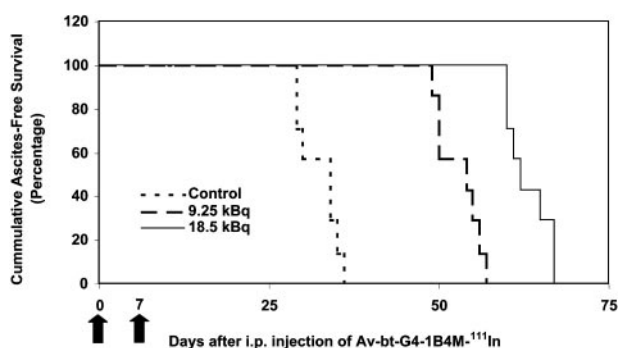


Fig. 4 Cumulative ascites-free survival curves for untreated and treated BALB/c nude mice bearing a peritoneal xenograft disseminated tumor. Treated mice received two i.p. injections of 9.25 and 18.5 MBq (groups A and B, respectively) of the  $[\text{Av-Bt-G4-(1B4M)}_{52}\text{-}^{111}\text{In}]_{\text{unsat}}$  compound. Short-dashed line, untreated mice; long-dashed line, 9.25 MBq-treated mice (group A); solid line, 18.5 MBq-treated mice (group B). Arrows indicate i.p. injection of the  $[\text{Av-Bt-G4-(1B4M)}_{52}\text{-}^{111}\text{In}]_{\text{unsat}}$  compound. Values were analyzed based on the data of seven mice for each group.

mice, even with the relatively low specific activity in the present experiment, a significant dose-dependent therapeutic effect was observed.

Several favorable points could be mentioned to advocate the use of Starburst PAMAM dendrimers in this study, including (a) the architecture of this molecule, which is composed by a regular dendritic branching and radial symmetry, and (b) the large number of surface amine groups that make this molecule highly positively charged (7, 8). These polycationic polymers can be used as a substrate for the attachment of multiple chelating agents to radioisotopes (8, 29, 30). Polycationic charges on the surface of the dendrimers interact electrostatically with negatively charged residues on the cell surface, and this electrostatic interaction is believed to facilitate the endocytosis process (31). Dendrimers appear to be highly efficient for *in vitro* transfection and are not cytotoxic at low concentrations

(31–33). For attachment of  $^{111}\text{In}$  on the dendrimer surface, we applied 1B4M as a chelate. The final product had 52 1B4Ms linked to a single G4 molecule, which can be used for attachment of  $^{111}\text{In}$ .

In the present biodistribution study, in addition to very high radioactivity uptake in the disseminated tumor with very low blood activity, we found relatively high uptake in normal organs such as liver, kidney, spleen, intestine, and stomach. High uptake in the stomach and intestine and to some extent in the spleen may be due to the radioactivity uptake in small disseminated tumors attaching on the surface of these organs. High uptake in the liver, kidney, and spleen was consistent with the report by Kobayashi *et al.* regarding the biodistribution of  $^{111}\text{In}$ -labeled PAMAM-1B4M-antibody conjugate (12, 29). By saturating the chelating sites on the Av-dendrimer conjugate, high uptake in these organs decreased, except for the kidney, and the high uptake in disseminated tumors also decreased. These findings have also been reported for dendrimers and dendrimer-antibody conjugates by Kobayashi *et al.* (12, 29). In their reports, the saturation of the chelating sites reduced the accumulation of the compounds especially in the kidney, liver, and spleen. Although no clear explanations of these findings have already been reported, they could be related to the difference in charge between unsaturated and saturated compounds. The charge of the unsaturated  $\text{G4-(1B4M)}_{52}$  is strongly negative, whereas saturated  $\text{G4-(1B4M)}_{52}$  is positively charged.

To facilitate the binding and internalization of this compound in the cancer cells, Av was chosen. Av is a basic glycoprotein with a molecular mass of  $\sim 67$  kDa and an isoelectric point of 10.5. It consists of four essentially identical subunits, each of which possesses a high affinity biotin-binding site (15, 16). The carbohydrate of Av contributed to its liver accumulation, and the positive net charge was related to its kidney accumulation (21). The relatively high uptake in the liver and kidney found in the biodistribution studies was due in part to this property of Av.

The carbohydrate moiety of Av has also been reported to facilitate the binding and internalization of compounds into

cancer cells by interaction with glycoprotein-binding receptors on the cancer cells (lectin; Ref. 20). Endogenous vertebrate lectins with galactoside-binding specificities have been detected in a wide variety of cells and tissues obtained from various species (34, 35). The presence of endogenous lectins in various tumor cells has been also reported, and these proteins are involved in adhesion, growth regulation, and metastasis (36). The level of cell surface lectins increases in cell variants or clones that exhibit a higher metastatic potential (36, 37). The interaction between Av and lectins on the surface of cancer cells is essential for the internalization of these compounds. The internalization assay demonstrated that significant amounts of these compounds internalized effectively during the first 24 h.

Indium-111, an Auger and CE emitter, decays by electron capture, with a physical half-life of 2.83 days, to stable  $^{111}\text{Cd}$ , thereby releasing approximately 15 electrons/decay (26, 38). The toxicity of  $^{111}\text{In}$  is considered to be mediated by Auger and CEs with energy ranging from a few to hundreds of keV (26, 38). The path length of Auger electrons (0.02–14  $\mu\text{m}$ ) is too short to reach the DNA if the nuclear decay does not occur within the nucleus (27, 28, 38). However, if  $^{111}\text{In}$  disintegrates close to the DNA, Auger electrons have a cytotoxic effect that is close to high LET radiation (28, 39–41). On the other hand, the path length for CEs (200–600  $\mu\text{m}$ ) is long enough to be effective even when disintegrating outside the nucleus (26, 38). However, biological effectiveness of  $^{111}\text{In}$  reduces to low LET radiation (26, 28).

In the present study, our results clearly show the capability of this compound to internalize specifically into the cancer cells, although the intracellular localization has yet to be determined. The biodistribution studies of saturated and unsaturated compounds demonstrated high concentration in i.p. disseminated tumors with high tumor:background ratios. In fact, myelosuppression may not be a critical problem with this compound, although no specific study on myelosuppression has been done in the present study. When high doses of this compound were i.p. injected into mice bearing i.p. disseminated tumor xenograft, a significant dose-dependent treatment effect was observed with no apparent side effects in the treated groups. The next goal of the study should be to determine which makes the major contribution to the therapeutic effect, Auger electron or CE.

In the present study, therapeutic dose of  $^{111}\text{In}$ -labeled compound was administered 5 days after i.p. injection of cancer cells, when only microscopic lesions have been formed. With regard to the very short path length of Auger and CEs, diffuse and homogeneous distribution of the radiolabeled compound in the tumor is important; this can be easily achieved for microscopic lesions, but it cannot be achieved for large lesions, where macromolecules cannot penetrate easily. Therefore, microscopic lesion seems to be the optimal candidate for internal radiation therapy using radionuclides with short path length.

In the present preliminary therapeutic experiment using  $^{111}\text{In}$ -labeled compound with relatively low specific activity, we could not completely control the formation of malignant ascites. However, with the use of radiolabeled compounds with much higher specific activities, we will be able to administer large amounts of radioactivities without increasing the protein dose of the compound and can expect a higher therapeutic effect.

In conclusion, we have successfully synthesized G4-Av

complex, which can be labeled with very high specific activity. The resulting radiolabeled compound accumulated highly and rapidly in i.p. disseminated tumor and internalized effectively. In addition, we have demonstrated that this compound could be used effectively for the treatment of i.p. disseminated tumors in BALB/c nude mice. Although the immunogenicity of Av may comprise the possible limitation (42, 43), this approach appears to be effective in treating peritoneal carcinomatosis of various malignancies.

## ACKNOWLEDGMENTS

We thank Japan Medipysics (Nishinomiya, Japan) for providing the  $^{111}\text{In}$  used in this study.

## REFERENCES

1. Daya, D., and McCaughey, W. T. Pathology of the peritoneum: a review of selected topics. *Semin. Diagn. Pathol.*, **8**: 277–289, 1991.
2. Chu, C. S., Menzin, A. W., Leonard, D. G., Rubin, S. C., and Wheeler, J. E. Primary peritoneal carcinoma: a review of the literature. *Obstet. Gynecol. Surv.*, **54**: 323–335, 1999.
3. Sugarbaker, P. H. Review of a personal experience in the management of carcinomatosis and sarcomatosis. *Jpn. J. Clin. Oncol.*, **31**: 573–583, 2001.
4. Hyams, D. M., Esteban, J. M., Lollo, C. P., Beatty, B. G., and Beatty, J. D. Therapy of peritoneal carcinomatosis of human colon cancer xenografts with yttrium 90-labeled anti-carcinoembryonic antigen antibody ZCE025. *Arch. Surg.*, **122**: 1333–1337, 1987.
5. Muto, M. G., Finkler, N. J., Kassis, A. I., Howes, A. E., Anderson, L. L., Lau, C. C., Zurawski, V. R., Jr., Weadock, K., Tumeh, S. S., Lavin, P., and Knapp, R. C. Intraperitoneal radioimmunotherapy of refractory ovarian carcinoma utilizing iodine-131-labeled monoclonal antibody OC125. *Gynecol. Oncol.*, **45**: 265–272, 1992.
6. Rosenblum, M. G., Verschraegen, C. F., Murray, J. L., Kudelka, A. P., Gano, J., Cheung, L., and Kavanagh, J. J. Phase I study of  $^{90}\text{Y}$ -labeled B72.3 intraperitoneal administration in patients with ovarian cancer: effect of dose and EDTA coadministration on pharmacokinetics and toxicity. *Clin. Cancer Res.*, **5**: 953–961, 1999.
7. Tomalia, D. A., Naylor, A. M., and Goddard, W. A., III. Starburst dendrimers: molecular-level control of size, shape, surface chemistry, topology, and flexibility from atoms to macroscopic matter. *Angew. Chem. Int. Ed. Engl.*, **29**: 138–175, 1990.
8. Wu, C., Brechbiel, M. W., Kozak, R. W., and Gansow, O. A. Metal-chelate-dendrimer-antibody constructs for use in radioimmunotherapy and imaging. *Bioorg. Med. Chem. Lett.*, **4**: 449–454, 1994.
9. Frechet, J. M. Functional polymers and dendrimers: reactivity, molecular architecture, and interfacial energy. *Science (Wash. DC)*, **263**: 1710–1715, 1994.
10. Barth, R. F., and Soloway, A. H. Boron neutron capture therapy of primary and metastatic brain tumors. *Mol. Chem. Neuropathol.*, **21**: 139–154, 1994.
11. Kobayashi, H., Kawamoto, S., Saga, T., Sato, N., Hiraga, A., Konishi, J., Togashi, K., and Brechbiel, M. W. Micro-MR angiography of normal and intratumoral vessels in mice using dedicated intravascular MR contrast agents with high generation of polyamidoamine dendrimer core: reference to pharmacokinetic properties of dendrimer-based MR contrast agents. *J. Magn. Reson. Imaging*, **14**: 705–713, 2001.
12. Kobayashi, H., Sato, N., Saga, T., Nakamoto, Y., Ishimori, T., Toyama, S., Togashi, K., Konishi, J., and Brechbiel, M. W. Monoclonal antibody-dendrimer conjugates enable radiolabeling of antibody with markedly high specific activity with minimal loss of immunoreactivity. *Eur. J. Nucl. Med.*, **27**: 1334–1339, 2000.
13. Sato, N., Kobayashi, H., Saga, T., Nakamoto, Y., Ishimori, T., Togashi, K., Fujibayashi, Y., Konishi, J., and Brechbiel, M. W. Tumor targeting and imaging of intraperitoneal tumors by use of antisense

- oligo-DNA complexed with dendrimers and/or avidin in mice. *Clin. Cancer Res.*, *7*: 3606–3612, 2001.
14. Yoo, H., Sazani, P., and Juliano, R. L. PAMAM dendrimers as delivery agents for antisense oligonucleotides. *Pharm. Res. (N. Y.)*, *16*: 1799–1804, 1999.
15. Green, N. M. Avidin. *Adv. Protein Chem.*, *29*: 85–133, 1975.
16. Hiller, Y., Gershoni, J. M., Bayer, E. A., and Wilchek, M. Biotin binding to avidin. Oligosaccharide side chain not required for ligand association. *Biochem. J.*, *248*: 167–171, 1987.
17. Kobayashi, H., Sakahara, H., Hosono, M., Yao, Z. S., Toyama, S., Endo, K., and Konishi, J. Improved clearance of radiolabeled biotinylated monoclonal antibody following the infusion of avidin as a “chase” without decreased accumulation in the target tumor. *J. Nucl. Med.*, *35*: 1677–1684, 1994.
18. Paganelli, G., Stella, M., Zito, F., Magnani, P., De Nardi, P., Mangili, F., Baratti, D., Veglia, F., Di Carlo, V., Siccardi, A. G., and Fazio, F. Radioimmunoguided surgery using iodine-125-labeled biotinylated monoclonal antibodies and cold avidin. *J. Nucl. Med.*, *35*: 1970–1975, 1994.
19. Zhang, M., Sakahara, H., Yao, Z., Saga, T., Nakamoto, Y., Sato, N., Nakada, H., Yamashina, I., and Konishi, J. Intravenous avidin chase improved localization of radiolabeled streptavidin in intraperitoneal xenograft pretargeted with biotinylated antibody. *Nucl. Med. Biol.*, *24*: 61–64, 1997.
20. Yao, Z., Zhang, M., Sakahara, H., Saga, T., Arano, Y., and Konishi, J. Avidin targeting of intraperitoneal tumor xenografts. *J. Natl. Cancer Inst. (Bethesda)*, *90*: 25–29, 1998.
21. Yao, Z., Zhang, M., Sakahara, H., Nakamoto, Y., Higashi, T., Zhao, S., Sato, N., Arano, Y., and Konishi, J. The relationship of glycosylation and isoelectric point with tumor accumulation of avidin. *J. Nucl. Med.*, *40*: 479–483, 1999.
22. Townsend, R., and Stahl, P. Isolation and characterization of a mannose/*N*-acetylglucosamine/fucose-binding protein from rat liver. *Biochem. J.*, *194*: 209–214, 1981.
23. Meredith, R. F., Khazaeli, M. B., Plott, W. E., Spencer, S. A., Wheeler, R. H., Brady, L. W., Woo, D. V., and LoBuglio, A. F. Initial clinical evaluation of iodine-125-labeled chimeric 17–1A for metastatic colon cancer. *J. Nucl. Med.*, *36*: 2229–2233, 1995.
24. Behr, T. M., Sgouros, G., Vougiokas, V., Memtsoudis, S., Gratz, S., Schmidberger, H., Blumenthal, R. D., Goldenberg, D. M., and Becker, W. Therapeutic efficacy and dose-limiting toxicity of Auger-electron vs. beta emitters in radioimmunotherapy with internalizing antibodies: evaluation of <sup>125</sup>I- vs. <sup>131</sup>I-labeled CO17-1A in a human colorectal cancer model. *Int. J. Cancer*, *76*: 738–748, 1998.
25. Saga, T., Sakahara, H., Nakamoto, Y., Sato, N., Zhao, S., Aoki, T., Miyatake, S., Namba, Y., and Konishi, J. Radioimmunotherapy of human glioma xenografts in nude mice by indium-111 labeled internalizing monoclonal antibody. *Eur. J. Cancer*, *35*: 1281–1285, 1999.
26. Griffiths, G. L., Govindan, S. V., Sgouros, G., Ong, G. L., Goldenberg, D. M., and Mattes, M. J. Cytotoxicity with Auger electron-emitting radionuclides delivered by antibodies. *Int. J. Cancer*, *81*: 985–992, 1999.
27. Behr, T. M., Behe, M., Lohr, M., Sgouros, G., Angerstein, C., Wehrmann, E., Nebendahl, K., and Becker, W. Therapeutic advantages of Auger electron- over beta-emitting radiometals or radioiodine when conjugated to internalizing antibodies. *Eur. J. Nucl. Med.*, *27*: 753–765, 2000.
28. Humm, J. L., Howell, R. W., and Rao, D. V. Dosimetry of Auger-electron-emitting radionuclides: report no. 3 of AAPM Nuclear Medicine Task Group No. 6. *Med. Phys.*, *21*: 1901–1915, 1994.
29. Kobayashi, H., Wu, C., Kim, M. K., Paik, C. H., Carrasquillo, J. A., and Brechbiel, M. W. Evaluation of the *in vivo* biodistribution of indium-111 and yttrium-88 labeled dendrimer-1B4M-DTPA and its conjugation with anti-Tac monoclonal antibody. *Bioconjug. Chem.*, *10*: 103–111, 1999.
30. Kobayashi, H., Kawamoto, S., Saga, T., Sato, N., Ishimori, T., Konishi, J., Ono, K., Togashi, K., and Brechbiel, M. W. Avidin-dendrimer-(1B4M-Gd)(254): a tumor-targeting therapeutic agent for gadolinium neutron capture therapy of intraperitoneal disseminated tumor which can be monitored by MRI. *Bioconjug. Chem.*, *12*: 587–593, 2001.
31. Kukowska-Latallo, J. F., Bielinska, A. U., Johnson, J., Spindler, R., Tomalia, D. A., and Baker, J. R., Jr. Efficient transfer of genetic material into mammalian cells using Starburst polyamidoamine dendrimers. *Proc. Natl. Acad. Sci. USA*, *93*: 4897–4902, 1996.
32. Bielinska, A., Kukowska-Latallo, J. F., Johnson, J., Tomalia, D. A., and Baker, J. R., Jr. Regulation of *in vitro* gene expression using antisense oligonucleotides or antisense expression plasmids transfected using starburst PAMAM dendrimers. *Nucleic Acids Res.*, *24*: 2176–2182, 1996.
33. Delong, R., Stephenson, K., Loftus, T., Fisher, M., Alahari, S., Nolting, A., and Juliano, R. L. Characterization of complexes of oligonucleotides with polyamidoamine starburst dendrimers and effects on intracellular delivery. *J. Pharm. Sci.*, *86*: 762–864, 1997.
34. Monsigny, M., Roche, A. C., and Midoux, P. Endogenous lectins and drug targeting. *Ann. N. Y. Acad. Sci.*, *551*: 399–413; discussion 413–44, 1988.
35. Gabius, H. J., Engelhardt, R., and Cramer, F. Endogenous tumor lectins: overview and perspectives. *Anticancer Res.*, *6*: 573–578, 1986.
36. Lotan, R. and Raz, A. Lectins in cancer cells. *Ann. N. Y. Acad. Sci.*, *551*: 385–396; discussion 396–398, 1988.
37. Raz, A., Meromsky, L., Zvibel, I., and Lotan, R. Transformation-related changes in the expression of endogenous cell lectins. *Int. J. Cancer*, *39*: 353–360, 1987.
38. Howell, R. W. Radiation spectra for Auger-electron emitting radionuclides: report No. 2 of AAPM Nuclear Medicine Task Group No. 6. *Med. Phys.*, *19*: 1371–1383, 1992.
39. McLean, J. R., Blakey, D. H., Douglas, G. R., and Bayley, J. The Auger electron dosimetry of indium-111 in mammalian cells *in vitro*. *Radiat. Res.*, *119*: 205–218, 1989.
40. McLean, J. R., and Wilkinson, D. The radiation dose to cells *in vitro* from intracellular indium-111. *Biochem. Cell Biol.*, *67*: 661–665, 1989.
41. Sahu, S. K., Kassis, A. I., Makrigiorgos, G. M., Baranowska-Kortylewicz, J., and Adelstein, S. J. The effects of indium-111 decay on pBR322 DNA. *Radiat. Res.*, *141*: 193–198, 1995.
42. Paganelli, G., Magnani, P., Zito, F., Villa, E., Sudati, F., Lopalco, L., Rossetti, C., Malcovati, M., Chiolerio, F., Seccamani, E., Siccardi, A. G., and Fazio, F. Three-step monoclonal antibody tumor targeting in carcinoembryonic antigen-positive patients. *Cancer Res.*, *51*: 5960–5966, 1991.
43. Chinol, N., Casalini, P., Maggiolo, M., Canevari, S., Omodeo, E. S., Caliceti, P., Veronese, F. M., Cremonesi, M., Chiolerio, F., Nardone, E., Siccardi, A. G., and Paganelli, G. Biochemical modifications of avidin improve pharmacokinetics and biodistribution, and reduce immunogenicity. *Br. J. Cancer*, *78*: 189–197, 1998.